Self-Assembly of Microtubules and Molecular Motors: Interaction of Polar Rods

Igor Aronson

Argonne National Laboratory

with

Lev Tsimring,
University of California, San Diego

Phys Rev E **71** 050901(R) 2005

Supported by the U.S. Department of Energy

Outline

- Introduction
- *in-vitro* experiments
- Review of recent theories
- Maxwell model for polar rods and granular analogy
- Asters and vortices
- Conclusion
- New systems

Microtubules

- Very long rigid polar hollow rods (length – 5-20 microns, diameter -40 nm, Persistent length – few mm)
- Length varies in time due to polymerization/depolymerization of tubulin
- Multiple function in the cell machinery: cytosceleton formation, cell division, cell functioning

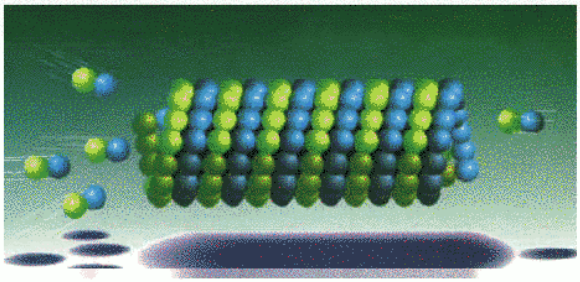

Molecular motors-Associated Proteins

- **Linear motors** (kinesin, dynein, myosin) cytosceleton formation, transport
- **Rotary motors:** (flagellar motor, F-ATPase) flagella rotation, ATP synthesis
- **Nucleic acid motors:** (helicase, topoisomerase) – DNA unwinding/translocation

Linear motors:

- Have one or two 'heads"
  - One attached to MT
  - Other attached to vesicles, granules, or another MT
- Take energy from hydrolysis of ATP
- Speed ~1μm/s, step length 8 nm, run length ~1μm
- Exert force about 6 pN

ATP – Adenosine triphosfate
ADP- Adenosine diphosphate

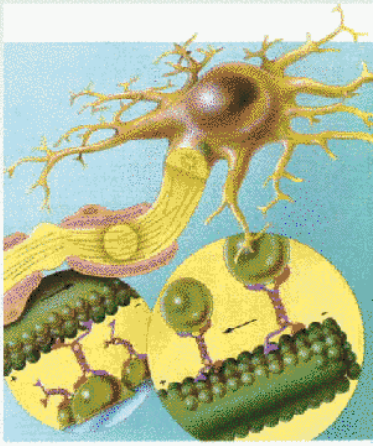

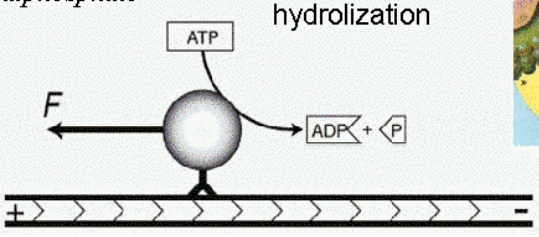

Simulations of MM motion

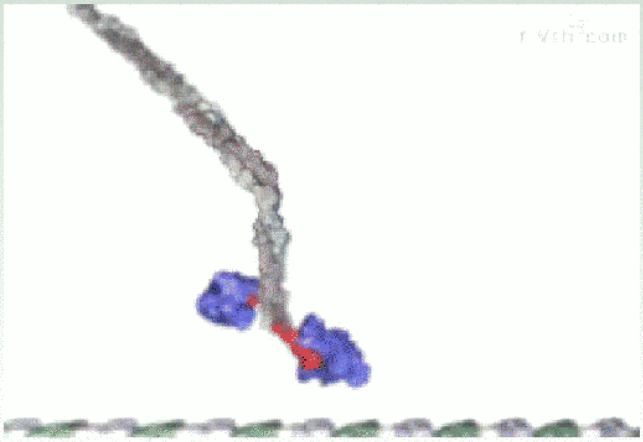

From Vale Lab, UC San Francisco
http://valelab.ucsf.edu

Dividing Cells and Miotic/Mitotic Spindles

- MT form cytosceleton of dividing cells
- Separate chromosomes

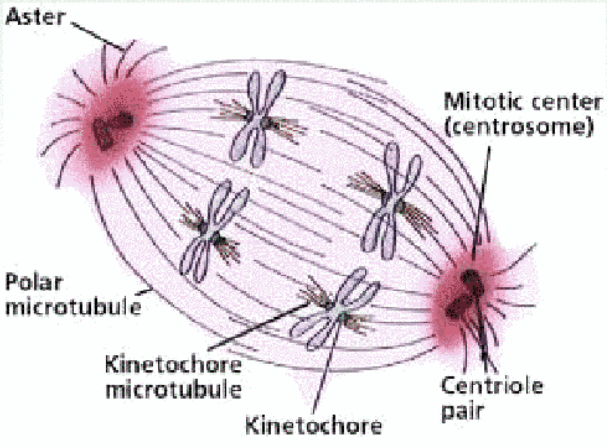

in-vitro Experiments with MT and MM

- Simplified system with only few purified components
- Experiments performed in 2D glass container: diameter 100 μm, height 5μm
- Controlled tubulin/motor concentrations and fixed temperature
- MT have fixed length 5μ due to fixation by taxol

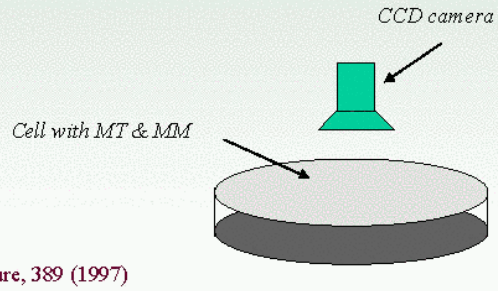

F. Nedelec, T. Surrey, A. Maggs, S. Leibler,
Self-Organization of Microtubules and Motors, Nature, 389 (1997)
T. Surray, F. Nedelec, S. Leibler & E. Karsenti,
Physical Properties Determining Self-Organization of Motors & Microtubules, Science, 292 (2001)
Y.Vugmeyster, E.Berliner, J.Gelles,
Release of Isolated Single Kinesin Molecules from Microtubules, Biochemistry 37, 747 (1998).
R.D.Vale, R.A.Milligan,
The way things move: looking under the hood of molecular motor proteins.Science 288, 88 (2000) 9

Single-molecule experiments

microtubule gliding on fixed kinesin
(R.D.Vale)

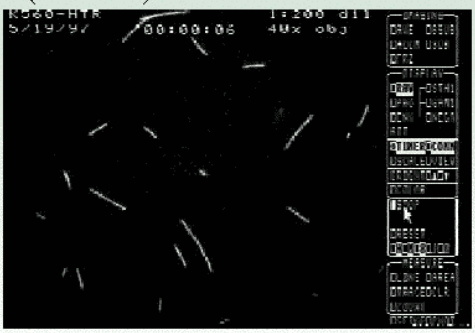

- http://valelab.ucsf.edu

kinesin moving a bead along MT
(Vugmeyster, Berliner, Gelles (1998))

http://www.bio.brandeis.edu/~gelles/

Patterns in MM-MT mixtures

Formation of asters, large kinesin concentration (scale 100 μ)

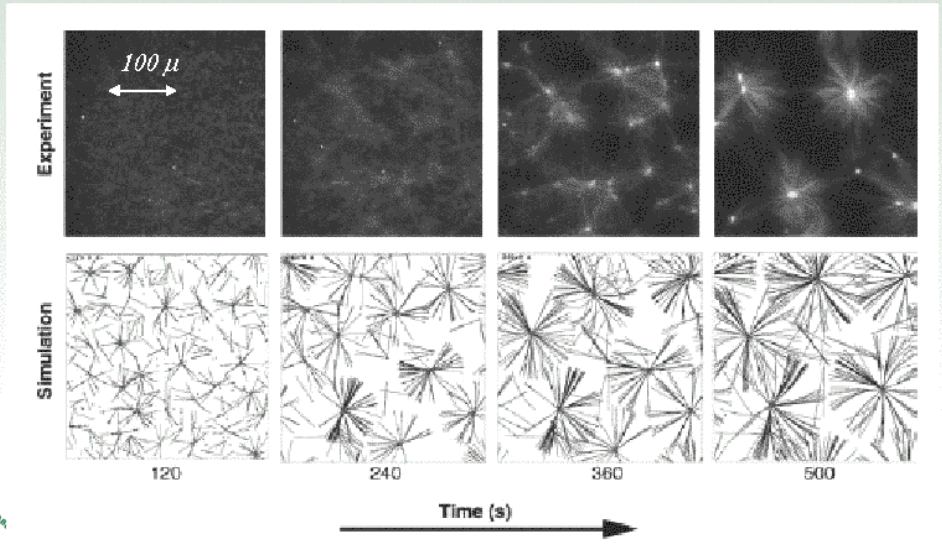

Vortex – Aster Transitions

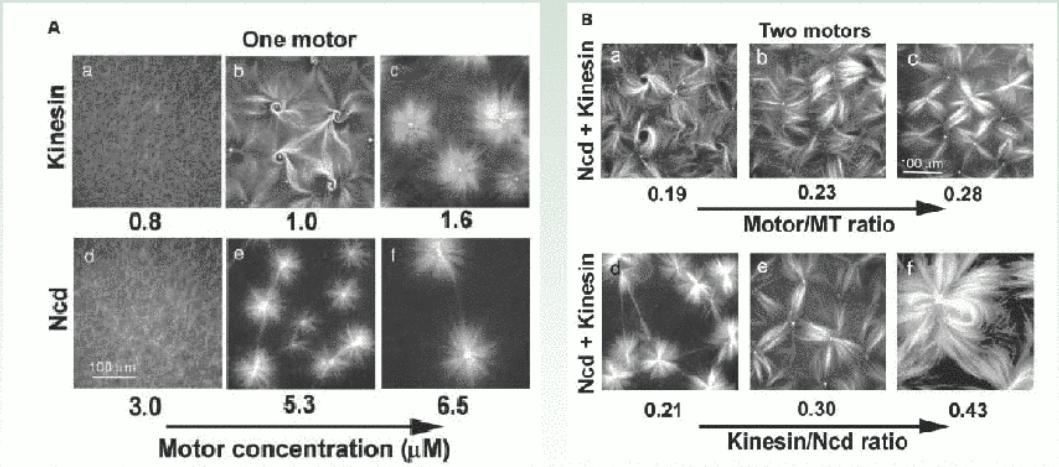

Ncd – gluthione-S-transferase-nonclaret disjunctional fusion protein
Ncd walks in opposite direction to kinesin

Dynamics of Aster/Vortex Formation

Kinesin

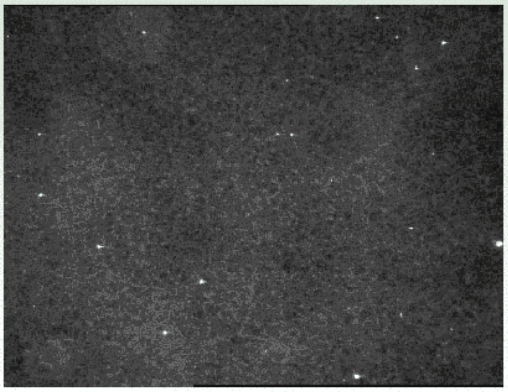

Ncd

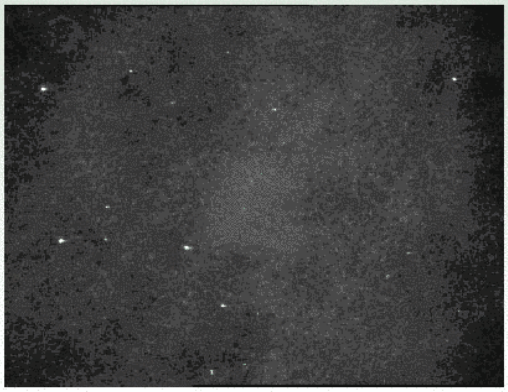

13

Rotating Vortex

Kinesin

14

Summary of Experimental Results

- 2D mixture of MM & MT exhibits pattern formation
- In kinesin vortices are formed for low density of MM and asters are formed for higher density
- In Ncd only asters are observed for all MM densities
- For very high MM density asters disappear and bundles formed

Mechanism of Self-Organization

Motor binding to 1 MT – no effect

Motor binding to 2 MT – mutual orientation after interaction

Zipper effect

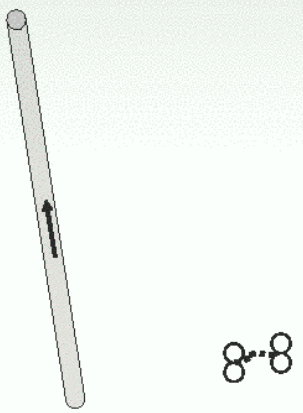

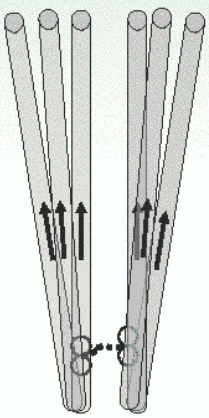

Review of theoretical results

- Lee & Kardar, PRE 64 (2001) – continuum phenomenological model for MM density and motor orientation
- Kruse, Joanny, Julicher, Prost, Sekimoto, PRL 92 (2004) – general phenomenological theory for active viscoelastic gels
- Liverpool and Marchetti, PRL 90 (2003) – continuum model derived from microscopic interaction roles

VOLUME 92, NUMBER 7 PHYSICAL REVIEW LETTERS week ending 20 FEBRUARY 2004

Asters, Vortices, and Rotating Spirals in Active Gels of Polar Filaments

K. Kruse,[1] J. F. Joanny,[2] F. Jülicher,[1] J. Prost,[2,3] and K. Sekimoto[2,4]
[1]*Max-Planck Institut für Physik komplexer Systeme, Nöthnitzerstrasse 38, 01187 Dresden, Germany*
[2]*Institut Curie, Section de Recherche, Physicochimie Curie (CNRS-UMR168), 26 rue d'Ulm 75248 Paris Cedex 05 France*
[3]*E.S.P.C.I., 10 rue Vauquelin, 75231 Paris Cedex 05, France*
[4]*LDFC Institut de Physique, 3 rue de l'Université, 67084 Strasbourg Cedex, France*
(Received 1 July 2003; published 20 February 2004)

The generalized flux-force relations for this problem read

$$2\eta u_{\alpha\beta} = \left(1 + \tau\frac{D}{Dt}\right) \times \left\{\sigma_{\alpha\beta} + \zeta\Delta\mu p_\alpha p_\beta + \bar{\zeta}\Delta\mu\delta_{\alpha\beta} - \frac{\nu_1}{2}(p_\alpha h_\beta + p_\beta h_\alpha) - \bar{\nu}_1 p_\gamma h_\gamma \delta_{\alpha\beta} + \tau A_{\alpha\beta}\right\}, \quad (1)$$

$$\frac{dp_\alpha}{dt} = -(v_\gamma\partial_\gamma)p_\alpha - \omega_{\alpha\beta}p_\beta - \nu_1 u_{\alpha\beta}p_\beta - \bar{\nu}_1 u_{\beta\beta}p_\alpha + \frac{1}{\gamma_1}h_\alpha + \lambda_1 p_\alpha\Delta\mu, \quad (2)$$

$$r = \zeta p_\alpha p_\beta u_{\alpha\beta} + \bar{\zeta}u_{\alpha\alpha} + \lambda\Delta\mu + \lambda_1 p_\alpha h_\alpha. \quad (3)$$

VOLUME 90, NUMBER 13 PHYSICAL REVIEW LETTERS week ending 4 APRIL 2003

Instabilities of Isotropic Solutions of Active Polar Filaments

Tanniemola B. Liverpool[1,3] and M. Cristina Marchetti[2,3]
[1]Applied Mathematics, University of Leeds, Leeds LS2 9JT, United Kingdom
[2]Physics Department, Syracuse University, Syracuse, New York 13244
[3]Kavli Institute of Theoretical Physics, University of California, Santa Barbara, California 93106

The filaments are modeled as rigid rods of length l and diameter $b \ll l$. Each filament is identified by the position $\mathbf{r}$ of its center of mass and a unit vector $\hat{\mathbf{n}}$ pointing towards the polar end. Taking into account *filament transport*, the normalized filament probability distribution function, $\Psi(\mathbf{r}, \hat{\mathbf{n}}, t)$, obeys a conservation law [13],

$$\partial_t \Psi + \nabla \cdot \mathbf{J} + \mathcal{R} \cdot \mathbf{J}^r = 0, \quad (1)$$

where $\mathcal{R} = \hat{\mathbf{n}} \times \partial_{\hat{\mathbf{n}}}$ is the rotation operator. The translational and rotational currents $\mathbf{J}$ and $\mathbf{J}^r$ are given by

$$J_i = -D_{ij}\partial_j \Psi - \frac{D_{ij}}{k_B T}\Psi \partial_j V_{ex} + J_i^{act}. \quad (2)$$

$$\partial_t \delta\rho = \frac{1}{d}[D_\parallel + (d-1)D_\perp](1 + v_0\rho_0)\nabla^2\delta\rho - \frac{\alpha l v_0 \rho_0}{12d}\nabla^2\delta\rho - \frac{\beta l^2 v_0 \rho_0 (2d+1)}{24d(d+2)}\nabla^2(\nabla \cdot \mathbf{t}), \quad (11)$$

$$\partial_t t_i = -D_r t_i + \frac{1}{d+2}[(d+1)D_\perp + D_\parallel]\nabla^2 t_i + \frac{2}{d+2}(D_\parallel - D_\perp)\partial_i \nabla \cdot \mathbf{t} - \frac{\alpha l v_0 \rho_0}{12d(d+2)}[\nabla^2 t_i + 2\partial_i \nabla \cdot \mathbf{t}] + \frac{\beta v_0 \rho_0}{d}\partial_i \delta\rho + \frac{\beta l^2 v_0 \rho_0 (2d+1)}{24d^2(d+2)}\partial_i \nabla^2 \delta\rho. \quad (12)$$

Maxwell Model for Inelastic Particles

in-elastic grains

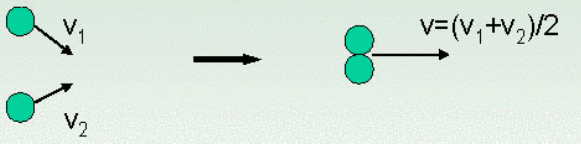

$$\begin{pmatrix} v_1^a \\ v_2^a \end{pmatrix} = \begin{pmatrix} \gamma & 1-\gamma \\ 1-\gamma & \gamma \end{pmatrix} \begin{pmatrix} v_1^b \\ v_2^b \end{pmatrix}$$

v^a & v^b velocities after/before collision
γ=0 – elastic collisions
γ=1/2 – fully inelastic collision
γ=*1* – no interaction

Probability distributions $P(v)$

- Collision rate g does not depend on relative velocity (Maxwell molecules)
- No spatial dependence
- D- thermal diffusion, $D \sim T$, T – temperature of heat bath
- Binary uncorrelated collisions

Distribution function for $\gamma=1/2$

source term *sink term*

$$\frac{\partial P(v)}{\partial t} = D\frac{\partial^2 P(v)}{\partial v^2} + g\int_{-\infty}^{\infty} du_1 \int_{-\infty}^{\infty} du_2 P(u_1)P(u_2)\left[\delta(v-(u_1+u_2)/2) - \delta(v-u_2)\right]$$

heat bath

Ben-Naim & Krapivsky, PRE 2000

Results for Maxwell Model

- Nice toy model: solution can be obtained analytically by the Fourier Transform of $P(v)$
- Asymptotic distribution $P(v)$ is localized but not Gaussian, the width depends on the temperature
- No phase transition, the diffusion can be scaled out

for $\gamma = \frac{1}{2}$

$$\frac{\partial P(v)}{\partial t} = \frac{\partial^2 P(v)}{\partial v^2} + \int_{-\infty}^{\infty} du \left[P(v+\tfrac{1}{2}u)P(v-\tfrac{1}{2}u) - P(v)P(v-u)\right]$$

Inelastic Collision of Polar Rods

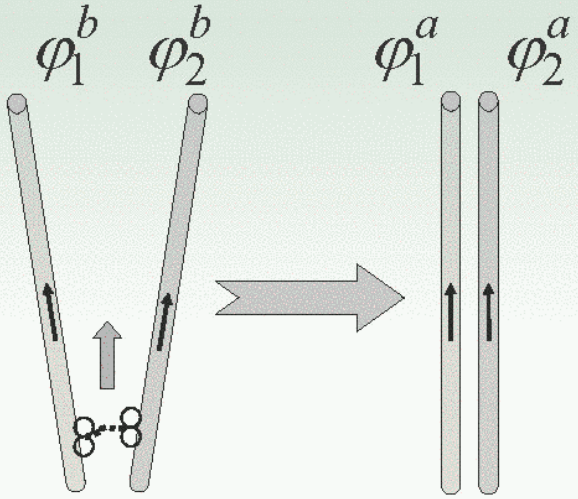

$$\varphi_1^a = \varphi_2^a = \frac{1}{2}\left(\varphi_1^b + \varphi_2^b\right)$$

$\varphi_{1,2}$ – orientation angles

Fully Inelastic Collision!!!

Probability distributions $P(\varphi)$

- D_r - thermal rotational diffusion
- g – collision efficiency (~ concentration of motors)
  since diffusion of motors >> diffusion of microtubules
  assume $g=const$

$$\frac{\partial P(\varphi)}{\partial t} = D_r \frac{\partial^2 P(\varphi)}{\partial \varphi^2} + g \int_{-\pi}^{\pi} du \left[P(\varphi + \tfrac{1}{2}u) P(\varphi - \tfrac{1}{2}u) - P(\varphi) P(\varphi - u)\right]$$

- Main difference – integration over finite interval due to 2π periodicity of the angle
- There is a phase transition as g increases!!!

Stability of disoriented state

- No preferred orientation: $P(\varphi)=P_0=1/2\pi$
- Small perturbations: $P(\varphi)=1/2\pi+\xi_n e^{\lambda t+in\varphi}+c.c.$

λ – growth-rate of linear perturbations

$$\lambda_1 = g\left(4/\pi - 1\right) - D_r$$

For $g>D_r/(4/\pi-1)\approx 3.662\, D_r$ - disoriented state loses stability

Orientation phase transition above critical motor density !!!

Macroscopic Variables

- Density of MT $\rho = 2\pi\langle P(\varphi)\rangle = \int_{-\pi}^{\pi} P(\varphi)d\varphi$

- Average orientation $\boldsymbol{\tau}=(\tau_x, \tau_y)$

$$\tau_x = \frac{1}{2\pi}\int_{-\pi}^{\pi}\cos\varphi P(\varphi)d\varphi \qquad \tau_y = \frac{1}{2\pi}\int_{-\pi}^{\pi}\sin\varphi P(\varphi)d\varphi$$

- "Complex orientation" $\psi = \tau_x + i\tau_y = \frac{1}{2\pi}\int_{-\pi}^{\pi} e^{i\varphi}P(\varphi)d\varphi$

Fourier Expansion

$$P(\varphi) = \sum_{n=-\infty}^{\infty} P_n e^{in\varphi}; \qquad P_n = \frac{1}{2\pi}\int_{-\pi}^{\pi} P(\varphi) e^{-in\varphi} d\varphi$$

Relation to observables

$$\rho = 2\pi P_0; \qquad \psi = P_{-1}; \qquad \psi^* = P_1$$

Asymptotic expansion for P_n (γ=1/2)

$$\dot{P}_k + (D_r k^2 + 1) P_k = 2\pi \sum_n \sum_m P_n P_m \frac{\sin[\pi(n-m)/2]}{\pi(n-m)/2} \delta_{n+m,k}$$

Scaling of variables $t \to D_r t; \qquad P_n \to \frac{g}{D_r} P_n$

- Diffusion $-D_r k^2$ forces rapid decay higher harmonics
- Linear growth rates λ_n

$$\lambda_0 = 0$$

$$\lambda_1 = \left(4/\pi - 1\right) - D_r > 0$$

$\lambda_n < 0$ *for* $|n| \geq 2$ Neglect higher harmonics

Asymptotic Landau Equation

- Truncation of series for $|n|>2$

$$\frac{\partial \rho}{\partial t} = 0$$

$$\frac{\partial \boldsymbol{\tau}}{\partial t} = \left(\left(\tfrac{4}{\pi} - 1\right)\rho - 1\right)\boldsymbol{\tau} - \frac{16\pi}{3(4+\rho)} |\boldsymbol{\tau}|^2 \boldsymbol{\tau} \approx \left(0.273\rho - 1\right)\boldsymbol{\tau} - 2.18 |\boldsymbol{\tau}|^2 \boldsymbol{\tau}$$

- Second order phase transition for $\rho>\rho_c = 1/0.273 \approx 3.662$

Second order phase transition for $\rho>\rho_c$

$$\frac{\partial \boldsymbol{\tau}}{\partial t} \approx \left(\rho / \rho_c - 1\right)\boldsymbol{\tau} - 2.18 |\boldsymbol{\tau}|^2 \boldsymbol{\tau}$$

$\rho<\rho_c$ – no preferred orientation
$|\boldsymbol{\tau}| \to 0$, stable point $\boldsymbol{\tau}=0$

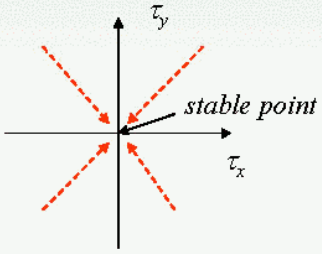

$\rho>\rho_c$ – onset of preferred orientation
$|\boldsymbol{\tau}| \to$ const, direction is determined by initial distribution, stable limit circle

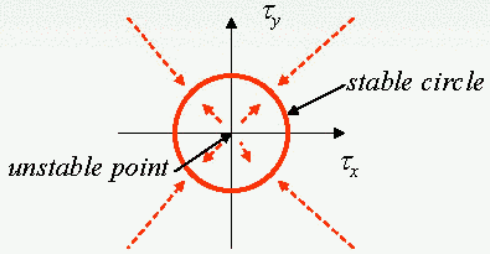

Compare with Hopf Bifurcation Scenario

Stationary Angular Distributions Comparison with Numerical Solution

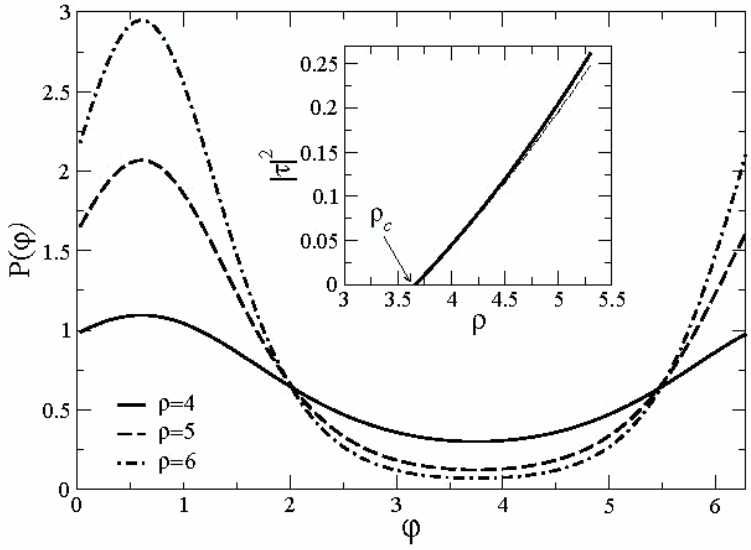

Spatial Localization of Interaction

- Interaction between rods decay with the distance
- Translational and rotational diffusion of rods

$$\frac{\partial P(\varphi, \mathbf{r})}{\partial t} = D_r \frac{\partial^2 P(\varphi, \mathbf{r})}{\partial \varphi^2} + \partial_i D_{ij} \partial_j P(\varphi, \mathbf{r}) + gI(W : P)$$

$I(W : P)$ – collision integral

W - interaction kernel

$D_{ij} = D_{\parallel} n_i n_j + D_{\perp}(\delta_{ij} - n_i n_j)$ – translational diffusion matrix

The Diffusion Matrix in Kirkwood Approximation

$$D_{ij} = D_{\|} n_i n_j + D_{\perp}(\delta_{ij} - n_i n_j) - \text{diffusion matrix}$$

$$\mathbf{n} = (\cos(\phi), \sin(\phi)) - \text{unit orientaional vector}$$

$$D_{\|} = k_B T \frac{\log(l/d)}{2\pi\eta_s l} - \text{parallel diffusion}$$

$$D_{\perp} = D_{\|}/2 - \text{perpendicular diffusion}$$

$$D_r = k_B T \frac{12\log(l/d)}{\pi\eta_s l^3} - \text{rotational diffusion}$$

l – length of the rod, d- diameter, η_s – viscosity of solvent

Interaction Kernel

- Decays with distance between rods
- Depends on relative angle between rods
- Symmetric with respect permutation of rods

$$W(\mathbf{r}_1, \mathbf{r}_2, \varphi_1, \varphi_2) = \frac{1}{\pi b^2} \exp\left[-\frac{|\mathbf{r}_1 - \mathbf{r}_2|^2}{b^2} \right] \left(1 + \beta(\mathbf{r}_1 - \mathbf{r}_2)(\mathbf{n}_1 - \mathbf{n}_2)\right)$$

$b = O(l)$ interaction scale

β characterizes anisotropy of interaction between polar rods

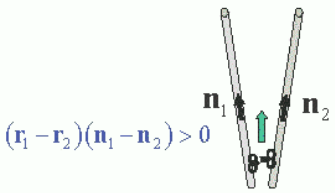

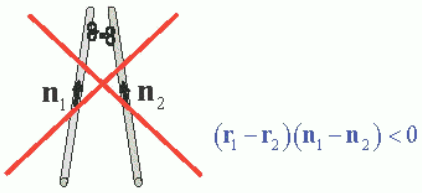

Collision Integral

$$I(W:P)=\iint d\mathbf{r}_1 d\mathbf{r}_2 \iint d\phi_1 d\phi_2 P(\phi_1,\mathbf{r}_1)P(\phi_2,\mathbf{r}_2)W(\phi_1,\mathbf{r}_1,\phi_2,\mathbf{r}_2)\times$$

$$\times\left[\delta(\mathbf{r}-(\mathbf{r}_1+\mathbf{r}_2)/2)\delta(\phi-(\phi_1+\phi_2)/2)-\delta(\mathbf{r}-\mathbf{r}_2)\delta(\phi-\phi_2)\right]$$

Continuum Equations

$$\frac{\partial\rho}{\partial t}=\nabla^2\left[\frac{\rho}{32}-\frac{B^2\rho^2}{16}\right]+\frac{\pi B^2 H}{16}\left[3\nabla\left(\boldsymbol{\tau}\nabla^2\rho-\rho\nabla^2\boldsymbol{\tau}\right)+2\partial_i\left(\partial_j\rho\partial_j\tau_i-\partial_i\rho\partial_j\tau_j\right)\right]-\frac{7B^4\rho_0\nabla^4\rho}{256}$$

$$\frac{\partial\boldsymbol{\tau}}{\partial t}=(0.273\rho-1)\boldsymbol{\tau}-2.18|\boldsymbol{\tau}|^2\boldsymbol{\tau}+\frac{5\nabla^2\boldsymbol{\tau}}{192}+\frac{\nabla\nabla\cdot\boldsymbol{\tau}}{96}+\frac{B^2\rho_0\nabla^2\boldsymbol{\tau}}{4\pi}+$$

$$+H\left[\frac{\nabla\rho^2}{16\pi}-\left(\pi-\tfrac{8}{3}\right)\boldsymbol{\tau}(\nabla\cdot\boldsymbol{\tau})-\tfrac{8}{3}(\boldsymbol{\tau}\nabla)\boldsymbol{\tau}\right]$$

$r\to\frac{r}{l}$ $\qquad B=\frac{b}{l}$ <1/2 normalized cuttoff length

$H=\frac{\beta b^2}{l}$ normalized kernel anisotropy

Term $\partial\rho_t\sim\nabla\rho\boldsymbol{\tau}+\ldots$ prohibited by the momentum conservation

Asters and Vortices

- For $HB^2 << 1$ equations split and become independent

$$\frac{\partial \boldsymbol{\tau}}{\partial t} = (0.273\rho - 1)\boldsymbol{\tau} - |\boldsymbol{\tau}|^2 \boldsymbol{\tau} + \frac{5\nabla^2 \boldsymbol{\tau}}{192} + \frac{B^2 \rho_0 \nabla^2 \boldsymbol{\tau}}{4\pi} + \frac{\nabla\nabla\cdot\boldsymbol{\tau}}{96} - H\left[0.321\boldsymbol{\tau}(\nabla\cdot\boldsymbol{\tau}) - 1.81(\boldsymbol{\tau}\nabla)\boldsymbol{\tau}\right]$$

- Without blue and red terms Eq possesses "Abrikosov Vortex Solution"

$$\psi = \tau_x + i\tau_y = F(r)\exp[i\theta + i\varphi]$$

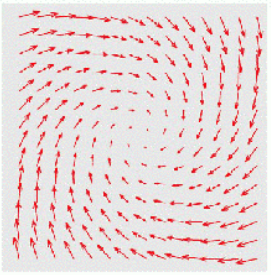

r, θ-polar coordinates

$\varphi = const$ arbitrary phase (tilt angle)

37

Vortices vs Asters

- For H=0 (no red terms) the only stable solutions $\varphi = \pm\pi/2$

Vortex: MT tilted off the center

Aranson & Tsimring, PRE 2003

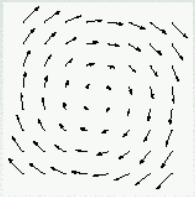

- For H≠0 (no blue terms) the only stable solution $\varphi = 0$

Aster: MT directed towards the center

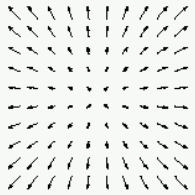

38

Vortex/Aster Solutions

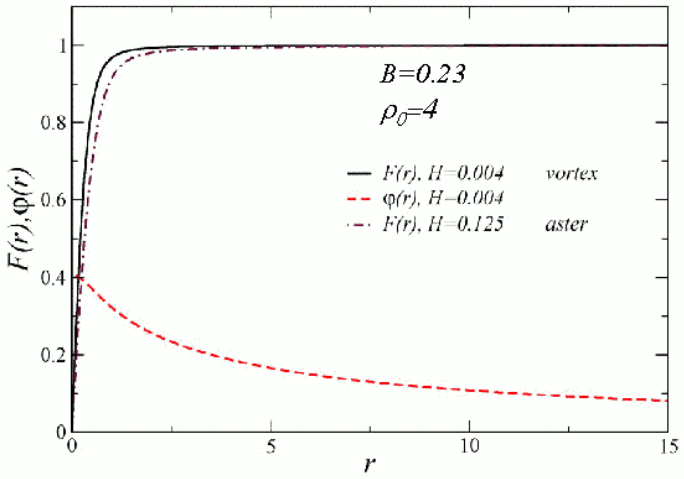

For H≠0 far away from the core the distinction between vortex and aster disappears

Linear Instability of Aster

$$\psi = \tau_x + i\tau_y = \left(F(r) + we^{\lambda t}\right)e^{i\vartheta}$$

r, ϑ – polar coordinates

F – aster solution function

w - linear perturbation

λ - linear growth rate

Linearized Equation for Aster

$$\lambda w = \left(D_{\parallel} - D_{\perp}\right)\Delta_r w + \left(1 - F^2 - 0.31 H \nabla_r F\right) w - 1.81 H F \nabla_r w$$

$$\Delta_r = \partial_r^2 + {}^{1}\!/_{r}\,\partial_r - {}^{1}\!/_{r^2}$$

$$\nabla_r = \partial_r + {}^{1}\!/_{r}$$

Equations solved numerically by shooting-matching method with Newton iterations

Phase Diagram

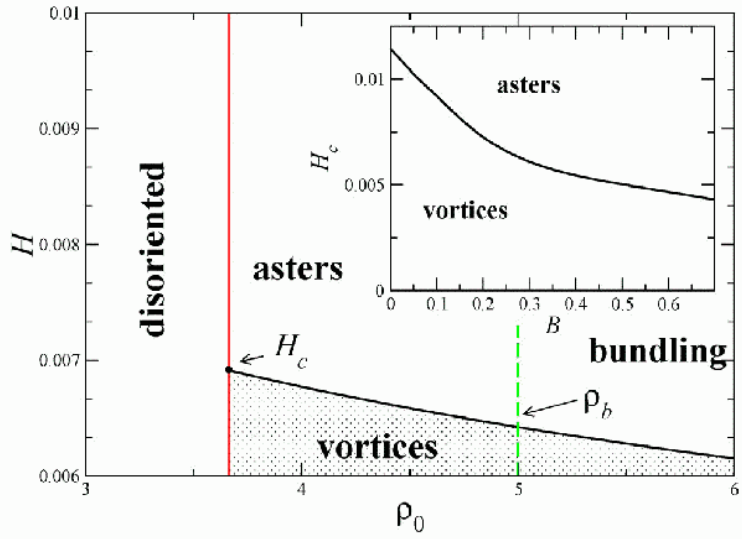

Implications of Analysis

- Asters stable for large MM density
- Vortices stable only for low MM density
- No stable vortices for $H>H_c$ for all MM density

(in experiments no vortices in Ncd for all densities)

Numerical Solution

- Quasispectral Method ; 256x256 FFT harmonics
- Periodic boundary conditions
- Spontaneous creation of vortices and asters

H=0.004

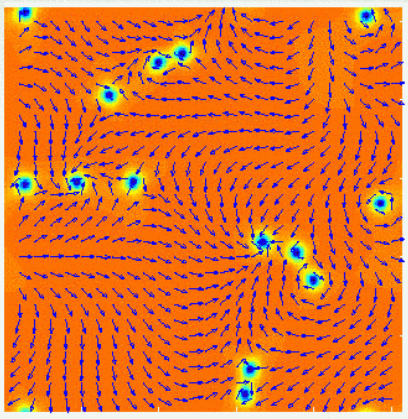

H=0.125

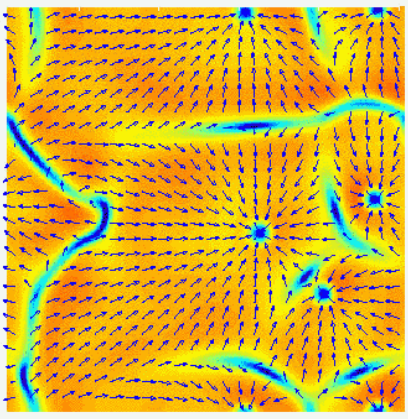

Evolution of Vortices and Asters

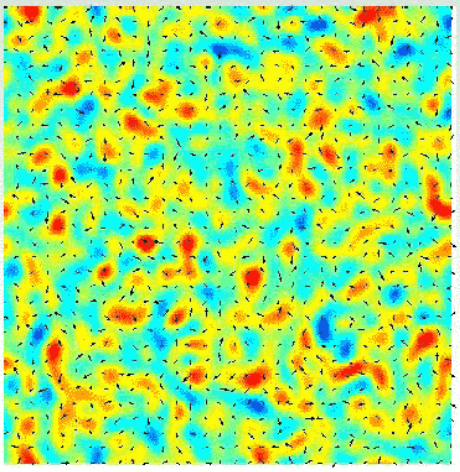

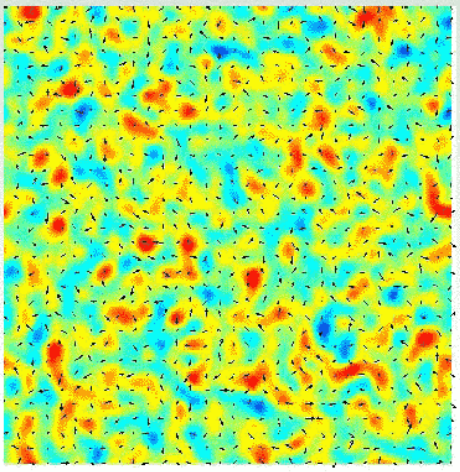

Conclusions

- Equations derived from microscopic model
- Reasonable agreement with experiment
- Possible applications for biological and non-biological systems:

  -biofilm formation by bacteria

  -organization of self-propelled particles (vibrated rods)

Blair-Kudrolli experiment

vibration of long rods

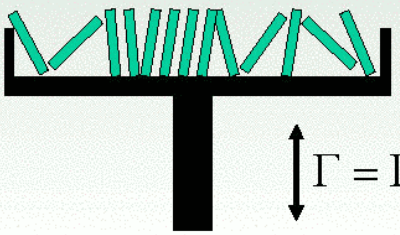

top view

long Cu cylinders
# of particles 10^4

51

Theoretical Description, I.A & L.T PRE (2003)

$$\partial_t \rho = -\frac{1}{\zeta}\nabla^2 \cdot \left(\nabla^2 \rho - \rho(1-\rho)(\delta-\rho)\right) + \alpha \nabla \cdot (\mathbf{n} f_0(n)(\rho+\rho_0))$$

$$\partial_t \mathbf{n} = f_1(\rho)\mathbf{n} - |\mathbf{n}|^2 \mathbf{n} + f_2(\rho)(\xi_1 \nabla^2 \mathbf{n} + \xi_2 \nabla\nabla \cdot \mathbf{n}) + \beta \nabla \rho$$

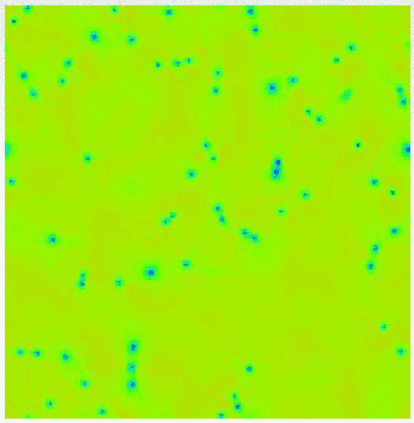

52

Self-propelled bioparticles

- swimming bacteriua *Bacillus subtilis*
- length 5 μm, speed 20 μm/sec
- collective flows up to 100 μm/sec

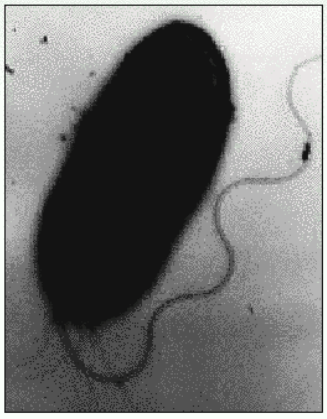

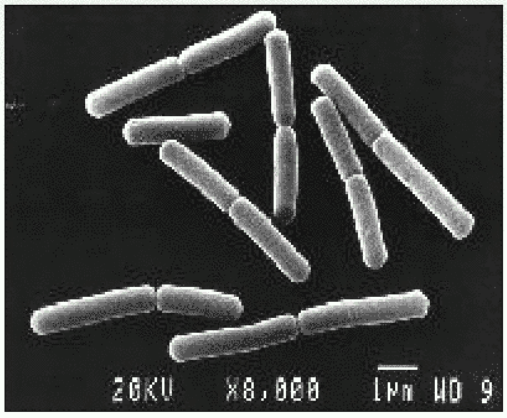

53

Turbulence in bacterial monolayer

- Experiment in fluid film (Andrey Sokolov and I.A. Argonne), collaboration with U Arizona (Ray Goldstein)
- Elementary interactions:
  -self-propulsion
  -hydrodynamic attraction (aka inelastic collision)
  -flow advection
  -direction realignment in shear flow

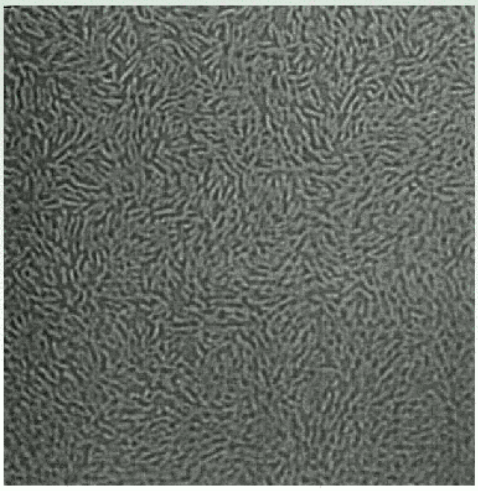

54

Theoretical model

- Ginzburg-Landau equation for orientation
- Coupled Navier-Stokes Equation for fluid velocity

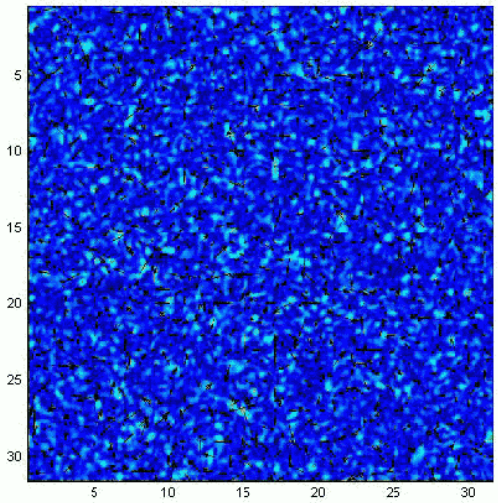

55